European Conference on Computational Fluid Dynamics
ECCOMAS CFD 2006
P. Wesseling, E. Oñate, J. Périaux (Eds)

A CONJUGATE HEAT TRANFER METHOD APPLIED TO TURBOMACHINERY

T. Verstraete*, Z. Alsalihi† and R. A. Van den Braembussche‡

* Von Karman Institute for Fluid Dynamics,
Waterloose steenweg, 72, 1640 Sint-Genesius Rode, Belgium
e-mail: tom.verstraete@vki.ac.be
Web page: http://www.vki.ac.be/

† ‡ Von Karman Institute for Fluid Dynamics,
Waterloose steenweg, 72, 1640 Sint-Genesius Rode, Belgium
e-mail: alsalihi@vki.ac.be, vdb@vki.ac.be

Key words: Conjugate Heat Transfer, Finite Element Analysis, Computational Fluid Dynamics, Coupled method, Turbomachinery

Abstract. *A Conjugate Heat Transfer (CHT) analysis allows the calculation of the heat transfer and temperature of a body placed in a fluid. The CHT analysis takes into account both the conduction in the solid and the convection in the fluid. Present paper describes a CHT method that uses two separate solvers: one CFD solver dedicated to the flow calculation and one Finite Element Analysis (FEA) solver for the computation of the heat transfer in the solid. Several methods, combining both codes in order to solve the CHT problem, are explained andevaluated. The CHT method is tested on two turbomachine applications.*

1 INTRODUCTION

The increase of power output and thermodynamic efficiency of gas turbines requires the turbine inlet temperature to be raised. In modern, high-performant gasturbines, the gas temperature often exceeds the melting point of the blade material. Cooling is applied to the airfoil to maintain the mechanical integrity. This particular example emphasizes the need for an accurate prediction of the heat transfer in turbomachinery. The blade solid temperature needs to be known in order to compute thermal stresses, creep, corrosion, maximum allowable stresses, etc. Moreover, in small gasturbines, heat transfer between the hot turbine and cold compressor can have an impact on the efficiency and therefore needs to be taken into account.

Most CFD predictions assume adiabatic conditions or constant surface temperature at the solid boundaries. The computational domain only includes the fluid. For the Conjugate Heat Transfer (CHT) method, the computational domain needs to be extended to the solid region. The heat conduction in the solid is included in the model and interaction at the common boundary between the fluid and structure solver is needed. Several approaches to solve the fluid structure interaction are discussed in present paper. A CHT method is applied to two turbomachinery applications. The first one consists of the hub cooling of an axial helium turbine blade. The maximum allowable temperature for the turbine disk material is defined from the expected life time. An accurate prediction of the heat transfer allows the calculation

of the required amount of cooling in the blade root.

The second application concerns the heat transfer analysis of a complete micro gasturbine, including compressor, turbine and stator. The high temperature difference between turbine and compressor in combination with the small dimensions results in a high heat transfer, causing a drop in efficiency of both components. The CHT analysis aims to quantify this heat transfer and to reveal the different mechanisms that contribute to it.

2 NUMERICAL METHOD

There are two main approaches to the conjugate heat transfer problem in turbomachinery[1-7]. One is by an extension of the CFD code to the solid region, where only the energy equation is solved. This method is mostly used and referred to in the literature as the conjugate method[3,6,7]. The main advantage is that only one code is needed for the whole domain. However, it requires modifications of the CFD code and grid generator.

The other approach is a coupling of two codes: a non-adiabatic Navier-Stokes (NS) solver for the flow in the fluid domain and a Finite Element Analysis (FEA) for the heat conduction in the solid. Continuity of temperature and heat flux at the common boundaries is obtained by an iterative adjustment of the boundary conditions. The advantage of the coupled approach is that one can use standard NS and FEA solvers and grid generators. Both codes have been extensively verified and their limitations and capabilities are well known. A FEA calculation is anyway needed for stress and vibration analysis. These have been the main arguments for using the coupled method in present study.

Disadvantages of the coupled method are the non-coinciding grids at the common boundary, requiring an interpolation to pass boundary conditions from one grid to the other and the need for an iterative procedure.

The non-adiabatic flow is calculated by means of TRAF3D[8]. This full 3D compressible Navier-Stokes solver uses a multi-stage Runge-Kutta time integration and central differencing with artificial dissipation applied to finite volumes. Convergence is accelerated by multigrid interpolation and implicit residual smoothing. The overall accuracy is second order at convergence. All calculations are done with the Baldwin-Lomax algebraic eddy-viscosity turbulence model. Despite its simplicity and low computational effort, good agreement with experiments is obtained for conjugate heat transfer as long as the flow is not separated[9]. The steady state heat transfer computation in the solid domain is predicted by the commercial FEA code SAMCEF[10] using quadratic tetrahedral elements.

2.1 Coupled method

The coupled method uses an iterative approach to obtain the same temperature and heat flux distribution at the boundaries that are common to the NS and FEA calculation domain. Fluid- and solid conduction computations alternate with an update of the boundary conditions in one of the following ways.

In a first method[5], the solid wall temperature distribution is imposed to the fluid solver and the heat flux distribution predicted by the fluid computation is imposed as a boundary condition to the solid conduction solver. This in turn predicts an updated temperature

distribution at the fluid solver solid boundaries. This loop is repeated until convergence i.e. when the temperature and heat flux are continuous between both domains. This method is known in the literature as the Flux Forward Temperature Back (FFTB) method, as the heat is given to the FEA calculation and the temperature is received back. However, imposing the heat flux on the entire boundary of the solid does not result in a unique solution. One must specify the temperature in at least one point of the domain.

Alternatively, one can also impose the heat flux distribution as a boundary condition for the fluid computation and the resulting wall temperature to the solid conduction solver. The updated heat flux is then returned as a boundary condition to the fluid solver. This method has been successfully applied by Heidmann[2] and is known as the Temperature Forward Flux Back (TFFB) method. The advantage of this method is that the temperature is given as a boundary condition to the FEA model, which is a more 'natural' boundary condition for the FEA heat transfer computation.

The main disadvantages of previous methods are a slow convergence and a risk of stability problems in areas of high temperature gradient.

The third method[4,5,11] uses the wall heat transfer equation (1) to update the boundary conditions.

$$q_W = h \cdot \left(T_W - T_{fl} \right) \tag{1}$$

It starts again with an initial guess of the temperature distribution T_w at the solid boundary of the flow solver. The results of the NS computation are used to estimate the heat transfer coefficient h and fluid temperature T_{fl} . Substituting them in (1) provides an implicit relation between T_w and q_w that can be used as a boundary condition for the solid conduction computation. The advantage of using (1) as boundary condition is an automatic adjustment of q_w as a function of the new T_w . The latter one is then returned to the fluid solver and the loop is repeated until convergence, i.e. until T_w and q_w are not changing anymore.

The remaining problem is the definition of h and T_{fl} from the NS solution. They also need to satisfy equation (1) in which T_w is the imposed boundary condition and q_w is the solution of the fluid solver. However, there is only one equation for two unknowns. One possibility is to make an extra fluid flow calculation with a different wall temperature[5] or even an adiabatic one[4]. Substituting the two solutions of q_w in (1) and assuming that h and T_{fl} remain unchanged provides equation (2) to define h.

$$h = \frac{q_{W1}^f - q_{W2}^f}{T_{W1}^f - T_{W2}^f} \tag{2}$$

T_{fl} can then be calculated by equation (1) in function of the imposed T_w and corresponding q_w. The difficulty is to ensure a positive value of h on the entire solid wall because negative values would make the conduction problem ill-posed[4]. They are likely to occur in regions where the heat flux is changing sign.

A simpler and more stable approach is by imposing a constant positive value of h. This is allowed because the value of h only influences the convergence rate. Following shows that it does not affect the final result.

The boundary conditions at iteration n are:

$$q_W^{f\,n} = h \cdot \left(T_W^{f\,n} - T_{fl}^{\,n} \right) \tag{3}$$

$$q_W^{s\,n} = h \cdot \left(T_W^{s\,n} - T_{fl}^{\,n} \right) \tag{4}$$

$$T_W^{f\,n+1} = T_W^{s\,n} \tag{5}$$

The first equation is used to compute, for a fixed value of h, the value of T_{fl} in function of the value T_w and q_w defined by the fluid computation. The second equation is the boundary condition for the conduction calculation in the solid. This results in a new T_w and q_w on the solid wall. The third equation defines the boundary condition for the next iteration of the fluid computation. Subtracting (4) from (3) gives:

$$q_W^{f\,n} - q_W^{s\,n} = h \cdot \left(T_W^{f\,n} - T_W^{s\,n} \right) \tag{6}$$

and substituting (5) results in:

$$q_W^{f\,n} - q_W^{s\,n} = h \cdot \left(T_W^{f\,n} - T_W^{f\,n+1} \right) \tag{7}$$

This means that if $\left| T_W^{f\,n} - T_W^{f\,n+1} \right| \to 0$ also $\left| q_W^{f\,n} - q_W^{s\,n} \right| \to 0$ and $\left| T_W^{f\,n} - T_W^{s\,n} \right| \to 0$

Hence the value of h has no effect on the solution once the continuity of temperature and heat flux between both domains is satisfied. It affects only the convergence history as can be seen from (7). A smaller value of h results in a larger change of the wall temperature between two successive iterations. This leads to a faster convergence but, as confirmed by the numerical experience, also leads to a less stable calculation. The choice of h is a trade off between computational time and stability.

The fluid computations between two successive solid calculations are not continued until full convergence. Full convergence of NS computations is useless as long as the boundary conditions are not correct. The NS computations are stopped after 100 pseudo-time steps to update the wall temperature by a solid conduction calculation. The choice of the number of NS iterations per solid-fluid iteration is driven by a minimization of the total CPU time. The number of pseudo-time steps should be high enough to obtain a modified boundary condition for the FEA code.

The initial guess of the wall temperature at the common boundary can be a uniform temperature, or the local fluid temperature of an adiabatic NS computation.

2.2 Interpolation between grids

Since the respective grids for the NS and FEA calculations are very different, the grid points at the common boundaries will not coincide. A NS solver needs small cells at boundaries where the velocity gradients are large. A FEA requires a finer grid distribution in areas of high curvature. Furthermore the NS solver defines the temperature in the cell center, while in the FEA the temperature is stored at the vertices of the elements. Hence two different

interpolations are necessary on the common wall. The T_{fl}, defined in the center of the NS cells, needs to be transferred to cell center of the FEA where the boundary condition (eq. 1) is applied. On the other hand, the temperature at the FEA vertices needs to be transferred to the cell center of the CFD cells. A distance-weighted interpolation based on Shapard's method[12] is used in both cases.

3 APPLICATION 1: AXIAL HELIUM TURBINE[13]

The axial helium turbine studied in present work is typical for the ones employed in direct cycle helium cooled nuclear reactors. Three blades are shown in figure 1. The aim of the study is to quantify the cooling needed at the hub of the blade in order to guarantee a rotor disk temperature not exceeding 750ºC. This is the maximum allowable blade disk material temperature imposed by the manufacturer for the required 60.000 hours lifetime. This maximum temperature is imposed at the bottom of the hub. The heat flux at the bottom of the hub is then the required cooling. The cooling can be obtained by cooling holes inside the hub, which are not modeled here.

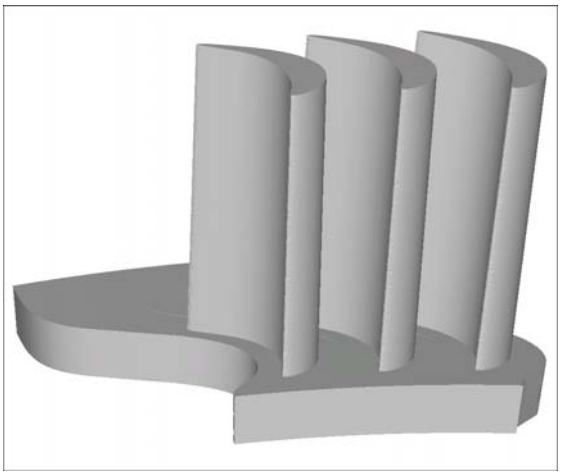

Figure 1: Three blades of the axial helium turbine. Cooling is applied at the bottom of the model (not shown)

3.1 Computational details

The Computational Fluid Dynamics (CFD) and Finite Element Method (FEA) domains are shown in figure 2 together with their boundary conditions. The regions of boundary condition information exchange between the CFD-FEA computations are shown by full thick lines.

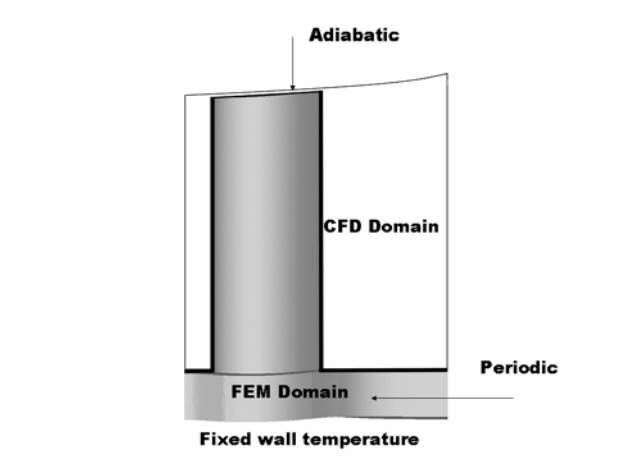

Figure 2: CFD and FEA model domains and
the boundary conditions in the meridional plane

Navier-Stokes computations are performed on one blade passage with periodicity boundary conditions in the circumferential direction. Total inlet pressure is 6.5 MPa and total inlet temperature is 1091.3 °K. The shroud is assumed to be adiabatic. The fluid is Helium which is treated as ideal gas with ideal gas constant R_{gas}=2078 kJ/(kg°K) and specific heat ratio of γ=1.666. The molecular Prandtl number is 0.6. For the turbulent Prandtl number 0.777 is used. The Reynolds number based on the total inlet conditions and axial chord is $11x10^6$.

The solid model consists of one blade and the 19.42mm thick hub plate. The turbine is made of Inconel which has a thermal conductivity of 30 W/(m. °K). The only fixed boundary condition imposed in the solid calculations is the fixed hub wall temperature. Periodicity in the blade-to-blade plane is also imposed in the FEA calculations.

The CFD grid has 120x52x52 cells in the streamwise, blade-to-blade and spanwise directions respectively. The FEA mesh consists of 330000 nodes and 230000 tetrahedral elements.

3.2 Results of the TFFB method

The model has been analyzed by means of two different CHT methods. The first analysis is done by the TFFB method. 120 iterations between CFD and FEA are performed. The small number of 10 pseudo time steps is used for each CFD calculation for stability reasons.

The convergence history of the method in terms of the maximum and rms norms of the temperature difference between two successive CFD analyses is shown in figure 3.

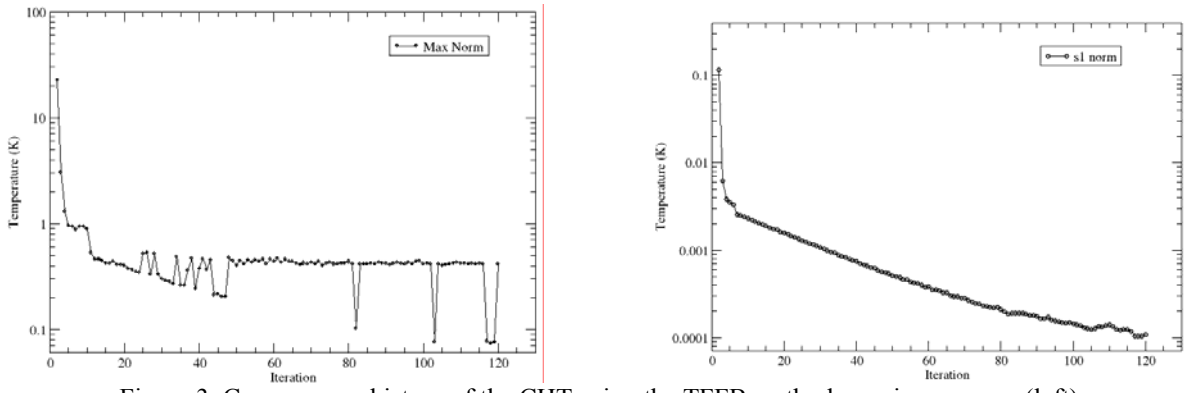

Figure 3. Convergence history of the CHT using the TFFB method: maximum norm (left) and rms norm (right) of the temperature difference between the CFD and FEA methods.

The final maximum temperature difference is 0.4 °K achieved after 120 Solid-Fluid iterations with the average RMS value below 10^{-4} °K. It is interesting to observe the oscillations in the maximum temperature norm. The TFFB method shows indeed stability problems and is not very robust. This has triggered the implementation of the so called h-method.

3.3 Results of the h-method

The second analysis is performed by the h-method. The constant value of h was taken to 80.000 W/(m^2ºK). This value is a trade off between computational time and stability. Smaller values lead to instabilities. The convergence history is given in figure 4. A sufficient small change in temperature (0.05 ºK) is achieved only after 30 iterations between CFD and FEA. Each CFD analysis consists of 100 pseudo time steps in order to achieve a reasonable changed CFD solution in a reasonable amount of time.

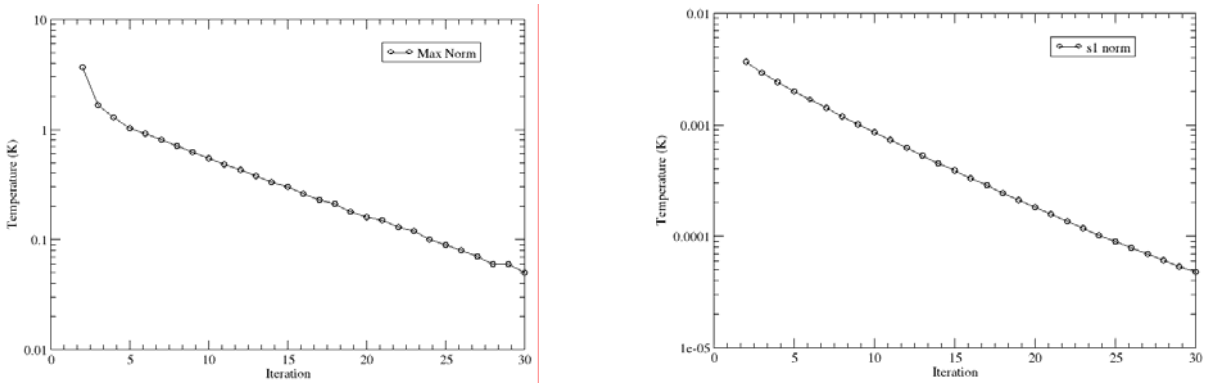

Figure 4. Convergence history of the CHT using the h-method: maximum norm (left) and rms norm (right) of the temperature difference between the CFD and FEA methods.

The h-method shows a much faster decrease in maximum norm and a significantly more

monotonic maximum residual reduction. The final wall temperature is already relatively well estimated after only one iteration as can be seen from figure 4 (left). Between the first and second temperature estimation of the FEA method, the maximum difference is less than 4 ºK.

The wall temperatures of the blades estimated by both methods are shown in figure 5. They compare well, although the temperatures calculated by the h-method are smoother.

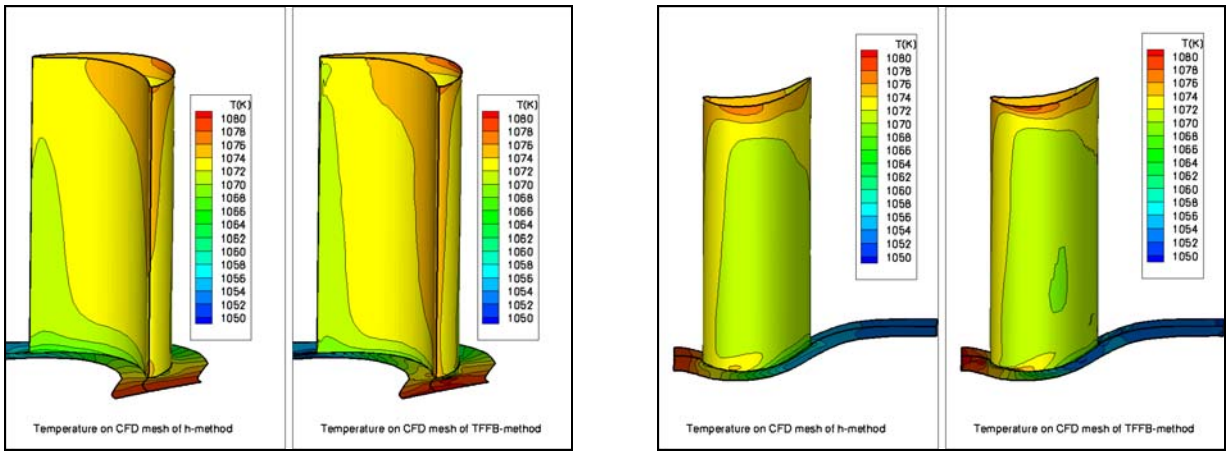

Figure 5. Comparison of the temperature on the blade surface using the h-method or TFFB method at pressure side (left) and suction side (right) of the blade.

The heat flux distributions on the blade calculated by FEA and CFD are compared in figure 6 for the h-method. As explained in 2.1, the h-method is not exchanging the heat flux at the common boundaries during the CHT analysis. However, at convergence both models should provide the same heat flux according to equation (7). Figure 6 shows that this constraint is almost satisfied for most of the regions, except for regions close to sharp corners. This is mainly due to the finite element representation of the convective boundary condition. Note also that in this particular case, h = 80.000, which means that a temperature difference of 0.05ºK obtained between the last two iterations already gives a difference in heat flux of 4.000 Watt/m^2. The high value of h is necessary because the computation is unstable at smaller values. Due to the use of helium as a fluid, small changes in wall temperature give large differences in heat flux and explain why this problem is very sensitive to variations in surface temperature.

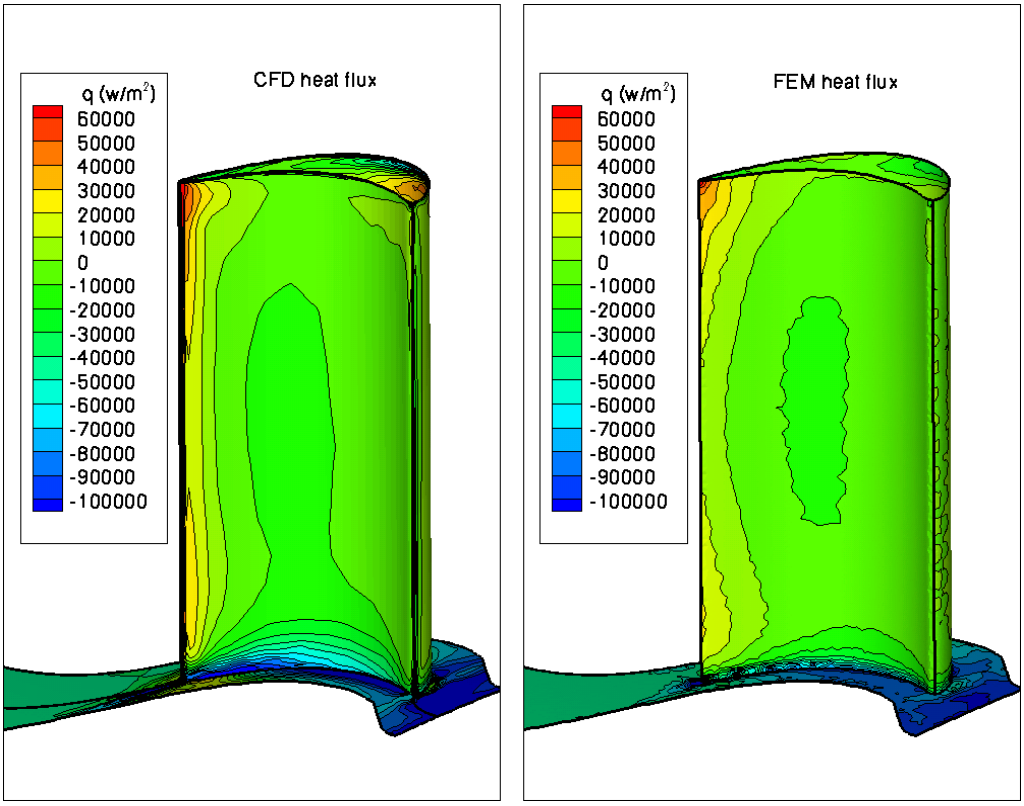

Figure 6.Heat flux distribution on the blade for the h-method.
Comparison of the heat flux computed by the CFD (left) and FEA (right).

4 APPLICATION 2: HEAT TRANSFER IN A MICRO GASTURBINE[14]

The last decade has seen a lot of research effort being oriented towards the development of micro gasturbines. Their potential for high power- and energy density makes them well suited to replace batteries in mobile applications. However, new problems arise when downscaling large turbomachines. They are related to machining, materials and the high heat transfer due to the high temperature differences over small distances. Adiabatic boundary conditions for the CFD calculations are no longer possible and a heat transfer calculation in the entire machine is necessary. This heat transfer is an important issue in the design of a micro gasturbine since it influences the efficiency of both compressor and turbine.

A good knowledge of the material temperature is also important since it influences corrosion, creep and maximum allowable stress. It is also needed to predict the thermal stresses and deformations of the individual components.

Figure 7 shows a schematic view on a micro gasturbine. It consists of a radial compressor

(left) and a radial turbine (right) mounted on one shaft. The diameter of the compressor and turbine is 20 mm, both components rotate at 500.000 rpm. The length of the shaft between compressor and turbine is 10 mm. Both rotor and stator are made of Kersit, which has a thermal conductivity of 28 W/(m.ºK).This ceramic material has been selected for its low density and for conserving its strength at high temperatures. This is needed because the small size of the components does not allow cooling.

4.1 Computational details

The computational domains are schematically shown on figure 8. Separate NS computations are made for the compressor-, turbine- and leakage flow between rotor and stator. Three FEA calculations are required: one respectively for the solid compressor, the turbine and the stator. Some simplifications have been implemented in order to obtain accurate results in a reasonable amount of CPU time.

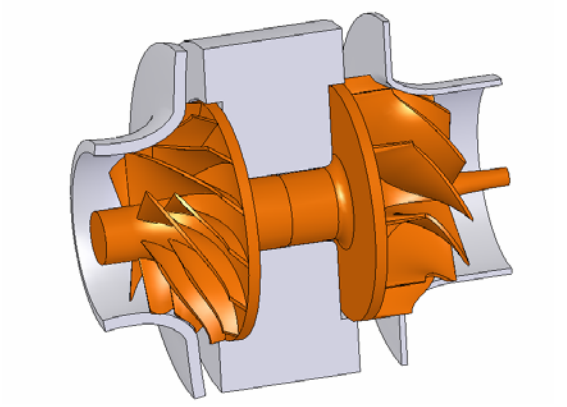

Figure 7. Micro gasturbine lay-out. Radial compressor (left) and turbine (right) are mounted on the same shaft

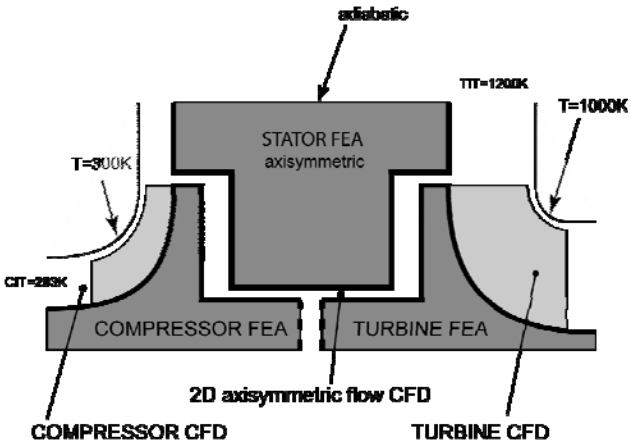

Figure 8. Numerial model of the micro gasturbine

Only conduction and convection are taken into account. Radiation is neglected since differences in surface temperatures are small. It has been calculated that the heat transfer due to radiation in the entire turbine is less than 1 Watt.

An axisymmetric temperature distribution is assumed in the stator. It constitutes a time-averaged boundary condition for the rotating components. Hence, the stator can be analyzed with a 2D axisymmetric model.

Adiabatic boundary conditions are imposed at the stator outer wall. This means that all the heat entering the stator from the turbine side is delivered to the compressor and clearance flow.

It is further assumed that the compressor and turbine shroud temperature are mainly defined by external conditions. The compressor shroud temperature is fixed at 300ºK which is close to the ambient temperature at compressor inlet. The proximity of the combustion chamber justifies a turbine shroud temperature of 1000ºK.

One can assume that the flow in the cavities and shaft clearance will be axisymmetric and can be analyzed with a 2D grid. The total inlet temperature and pressure are equal to the compressor rotor exit values. The exit pressure for the leakage flow is equal to the turbine leading edge static pressure. The inlet and outlet conditions for the leakage flow are updated only after the first iteration of the conjugate heat transfer calculation and remain constant for the rest of the computation. The 2D grid of the leakage flow inlet section has been axially extended to create a realistic inlet flow velocity profile. However the heat transfer is calculated only starting from the rim of the compressor disk.

Only one periodic part of the compressor and turbine is analyzed imposing periodic boundary conditions in both solid and fluid calculations. The NS calculations of the compressor and turbine interact with the FEA computations for rotor and stator. The value of wall temperature and T_{fl} are passed between both grids by a regular interpolation as explained previously. The surfaces where the NS and FEA exchange boundary conditions are marked with a thick line in figure 8. The boundary conditions for the 2D stator- and clearance gap calculations are the circumferentially averaged values of the 3D impeller flow. A circumferential averaging of the 3D results followed by a 2D interpolation define the boundary conditions for the 2D calculation. The uniform conditions on the shrouds and the results of the 2D stator- and clearance gap calculations correspond to a time averaged boundary conditions for the 3D calculations.

The difference in periodicity between the turbine ($2\pi/10$) and the compressor ($2\pi/7$) requires a separate FEA for both components. Continuity of temperature and heat flux at the common boundary, marked with a thick dashed line on figure 8, is obtained by an iterative update of the temperature. After each FEA analysis, the heat flux at the interface is compared, taking into account the difference in cross section. Any difference between them will give rise to a modified temperature on the interface defined by:

$$T_{new} = T_{old} + C \cdot (q_w^{comp} + q_w^{turb}) \tag{8}$$

Positive values of q_w correspond to heat fluxes leaving the solid. C in formula (8) is a positive value fixed at 1E-5 $^oK.m^2/W$. More heat leaving the turbine than going in the compressor will lead to an increase of the interface temperature. The turbine heat flux will decrease and more heat will enter the compressor. Higher values of C favor convergence but decrease stability.

The compressor NS grid contains 840.000 cells; the FEA compressor and turbine grid have each 180.000 elements and 275.000 nodes. The turbine NS grid contains 590.000 cells. The 2D FEA grid for the stator has 20.000 elements and the leakage flow is modeled on a 2D grid with 10.000 axisymmetric cells.

Calculations are run in parallel on three CPU's. One is dedicated to the compressor, one to the turbine and the third one calculates the gap flow and stator heat transfer. Each CPU switches between a NS and FEA calculation for one part of the model. The convection

coefficient h is set to 3000. A typical convergence history of the temperatures L^{∞} residuals ($\left|T^{s\,n+1} - T^{s\,n}\right|_{\max}$) is plotted in figure 9. Convergence of the entire model is obtained after ~20 solid-fluid iterations. Each Ns computation consists of 100 pseudo time steps.

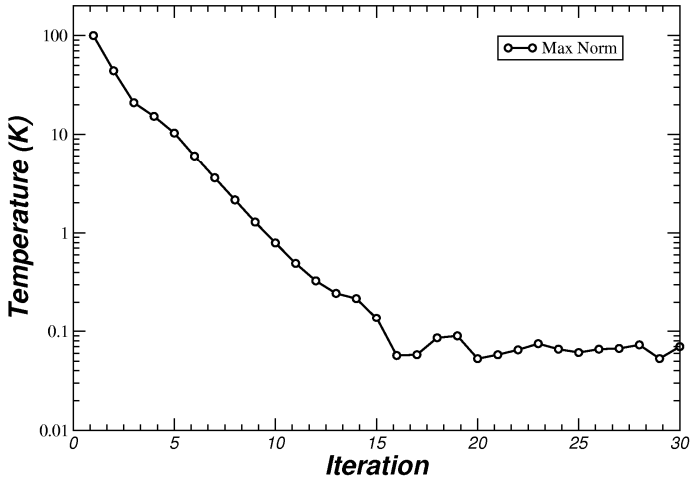

Figure 9. Convergence history of L^{∞}

4.2 Results

The temperature distribution in the solid is shown in figure 10. More detailed views of the temperature distribution in the compressor and turbine are shown in figures 11 and 12. A large temperature difference is observed between the compressor and turbine impeller. In spite of this, only a small amount of heat from turbine to compressor is predicted, see figure 13 and table 1. One part of this heat transfer is going trough the shaft. The shaft thermal resistance, defined by $\lambda \cdot \pi d^2 / l$, equals 0.079 W/ºK. This explains why a 316 ºK temperature difference is needed to pass 25 W through the shaft of 10 mm length. Only a small amount of heat is going from the shaft to the leakage flow.

The second contribution to the heat transfer is by the air passing trough the back of the compressor and turbine disks. It is influenced by the thermal resistance of the stator and the flow in the gap. The thermal resistance of the stator is much smaller than the one of the rotor since it has a much bigger cross section. The main resistance for the second heat flux thus results from the flow in the cavity.

The pressure difference between the compressor exit and turbine inlet defines the leakage flow from the compressor to the turbine. This flow acts like a coolant, taking away heat from the stator and rotor. The flow pattern in the cavities behind the compressor and turbine are visualized in figure 14 together with the total temperature distribution. The flow is centrifuged outwards near the impeller and driven inwards near the stator by the radial pressure gradient. This recirculation not only enhances the heating by disk friction losses but also favors the heat transfer in the cavity. Part from the flow heated at the stator wall of the compressor cavity is recirculated and heats the compressor hub disk. In the turbine cavity, the flow heated on the

hub disk leaves the cavity at the turbine leading edge. Note that the computed flow in the cavity is a 3D flow, but in figure 13 only two velocity components are visualized. The velocity profile perpendicular to the figure is not shown.

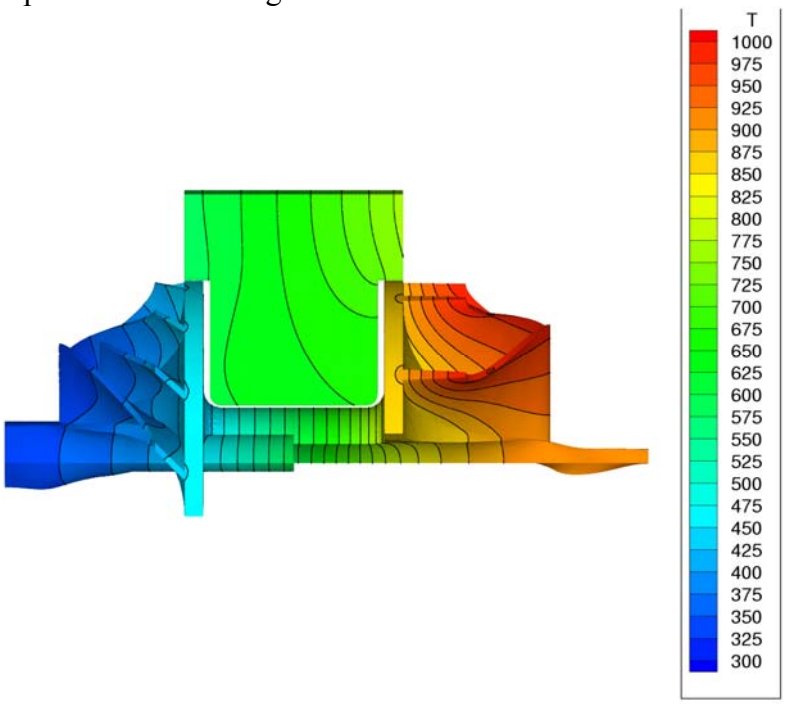

Figure 10. The temperature distribution in the rotor and stator.

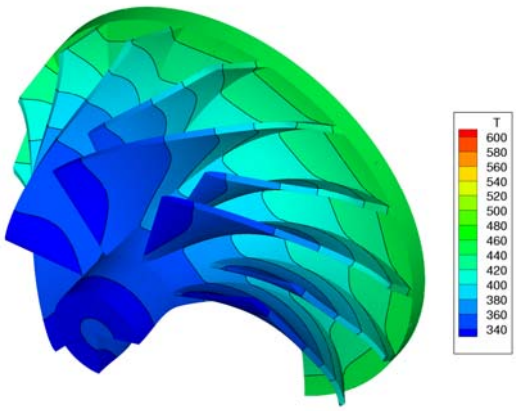

Figure 11. Detail of the temperature distribution of the compressor. Temperatures are in ºK.

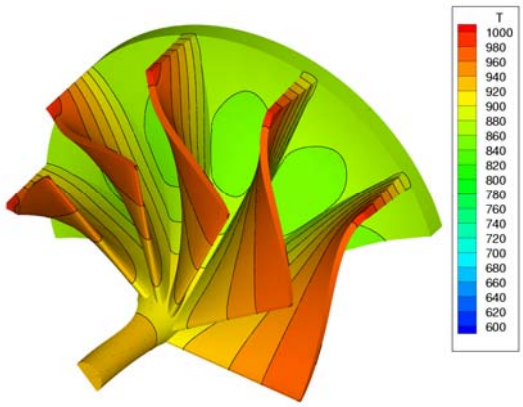

Figure 12. Detail of the temperature distribution of the turbine. Temperatures are in ºK.

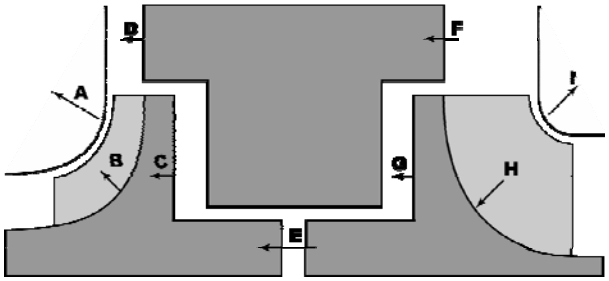

Figure 13. Heat transfer in the micro gasturbine

	Heat (W)
A	217
B	76
C	35
D	140
E	25
F	208
G	46
H	85
I	95

Table 1. Heat transfer in the micro gasturbine

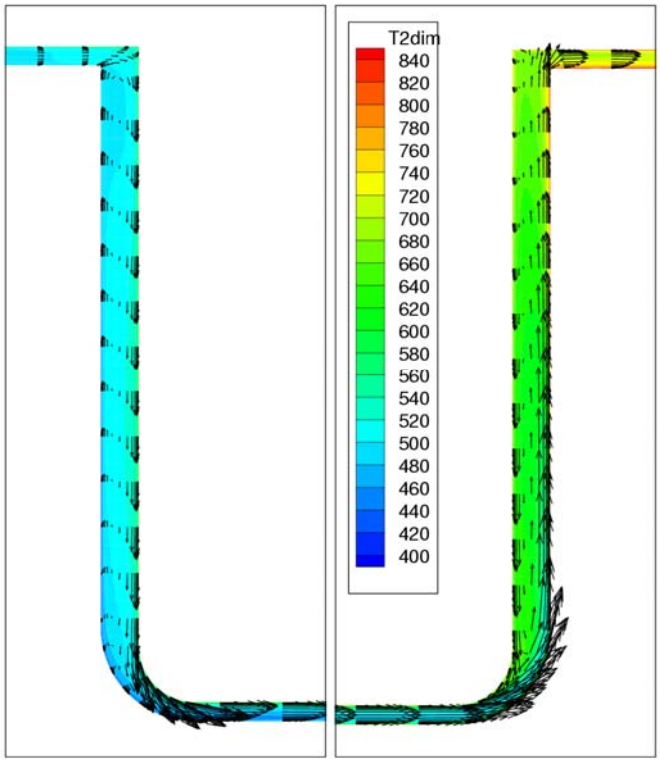

Figure 14. Total temperature (ºK) and flow field in the compressor (left) and turbine (right) cavity. Temperatures are in ºK.

5 CONCLUSIONS

A conjugate heat transfer method was developed and applied on two turbomachinery applications. Different coupling methods have been evaluated and it is shown that the so called h-method is the most robust and shows the best convergence rate.

The other benefit of the presented method is related to the coupling of standard and well proven CFD and FEA solvers. The CFD code does not have to be extended to the solid domain.

The computational time for a CHT calculation takes up to 5 times longer with respect to a sole CFD computation, but the additional information on heat transfer and material temperature are worth this extra time. The FEA method can provide other useful information such as thermal and centrifugal stresses with a minimum of extra effort.

6 ACKNOWLEDGEMENTS

This research is sponsored by the IWT, the Institute for the Promotion of Innovation by Science and Technology in Flanders, Belgium, project SBO 030288 "PowerMEMS".

7 REFERENCES

[1] Bohn, D., Bonhoff, B., and Schonenborn, H., "Combined Aerodynamic and Thermal Analysis of a Turbine Nozzle Guide Vane"' IGTC paper 95-108.
[2] Heidmann, J. D., Kassab, A. J., Divo, E. A., Rodriguez, F. and Steinthorsson, E., "Conjugate Heat Transfer Effects on a Realistic Film-cooled Turbine Vane", ASME paper GT2003-38553.
[3] Han, Z.-X., Dennis, B. H. and Dulikravich, G. S., "Simultaneous Prediction of External Flow-Field and Temperature in Internally Cooled 3-D Turbine Blade Material", ASME paper 2000-GT-253.
[4] Montenay, A., Paté, L. and Duboué, J., "Conjugate Heat Transfer Analysis of an Engine Internal Cavity", ASME paper 2000-GT-282.
[5] Verdicchio, J. A., Chew, J. W. and Hills, N. J., "Coupled Fluid/Solid Heat Transfer Computation for Turbine Discs", ASME paper 2001-GT-0205.
[6] York, W. D. and Leylek, J. H., "Three-Dimensional Conjugate Heat Transfer Simulation of An Internally-Cooled Gas Turbine Vane", ASME paper GT2003-38551.
[7] Bohn, D., Heuer, T. and Kusterer, K., Conjugate Flow and Heat Transfer Investigation of a Turbo Gharger: Part I: Numerical Results", ASME paper GT2003-38445.
[8] Arnone, A., "Viscous analysis of Three-Dimensional Rotor Flow Using a Multigrid Method", ASME Journal of Turbomachinery, Vol. 116, pp 435-445.
[9] Grag, V. K., "Heat Transfer Research on Gas Turbine Airfoils at NASA GRC", International Journal of Heat and Fluid Flow 23 (2002), pp 109-136.
[10] SAMCEF FEA code by Samtech Group, www.samcef.com.
[11] Lassaux, G., Daux, S. and Descamps, L., "Conjugate Heat Transfer Analysis of a Tri-Dimensional Turbine Blade Internal Cavity", 24th ICAS 2004.
[12] Shepard, D., "A Two-Dimensional Interpolation Function for Irregularly Spaced Data", Proc. 23rd ACM National Conference (1968) pp 517-524.
[13] Verstraete, T., Alsalihi Z., and Van den Braembussche R. V. A., 2006, "Numerical Study of the Heat Transfer in an Axial Helium Turbine" , Proceedings of CMFF'06: The 13th International Conference on Fluid Flow Technologies, September 6-9, 2006, Budapest, Hungary.
[14] Verstraete, T., Alsalihi Z., and Van den Braembussche R. V. A., 2006, "Numerical Study of Heat Transfer in Micro Gas Turbines", ASME paper GT2006-90161.